Earthquake Engineering, Tenth World Conference © 1992 Balkema, Rotterdam. ISBN 90 5410 060 5

Hysteretic analysis of composite beam-to-column joints

W.Kim
SAC International, Ltd, Seoul, Korea

L.-W.Lu
Lehigh University, Bethlehem, Pa., USA

ABSTRACT: The behavior and strength of composite beam-to-column joints subjected to monotonic and cyclic shear is examined. Analytical models defining the shear force and shear deformation relationship of joint panels have been developed by applying structural mechanics principles and results of previous experimental studies. The concept of superposition of the contributions of steel and reinforced concrete panels is utilized in the development. The force-deformation relationships predicted by the models show good agreement with test results in terms of strength, stiffness and energy dissipation capacity. These models have already been implemented in a computer program capable of performing inelastic seismic response analysis of building systems.

1 INTRODUCTION

When a moment- resisting frame is subjected to seismic loads, its beam-to-column joints undergo considerable angular deformation due to large shear force transmitted to the joints. In order to perform inelastic seismic analyses of such frames, it is necessary to know the complete joint force-deformation relationship.

Monotonic and hysteretic behavior of steel beam-to-steel column joints has been investigated in a number of extensive experimental and analytical research programs. The recent studies have concluded that the joints develop their shear strength from yielding and strain hardening of the joint web panel and bending of the column flanges and they generally exhibit excellent ductile behavior.

Similarly, the monotonic and hysteretic behavior of reinforced concrete beam-to-column joints has been investigated. Most of the analytical research was based on a strut model utilizing the diagonal compression field of concrete and the tension force in reinforcing bars.

The monotonic and hysteretic behavior of composite beam-to-composite column joints has been investigated in Japan by Minami (1986), Nishimura, et al (1986, 1987) and Matsui, et al (1987). These studies show that the shear strength of composite joints can be predicted by superposing the contributions of the steel and reinforced concrete panels and that column axial compression does not significantly affect the shear strength. No rational monotonic or hysteretic model defining the force-deformation relationships of the joints has been developed.

2 INELASTIC ANALYSIS OF JOINT BEHAVIOR

Figure 1 shows a generic composite beam-to-column joint. The beam section is shown as an encased composite beam since most of the past tests were conducted on joints with encased beams. The

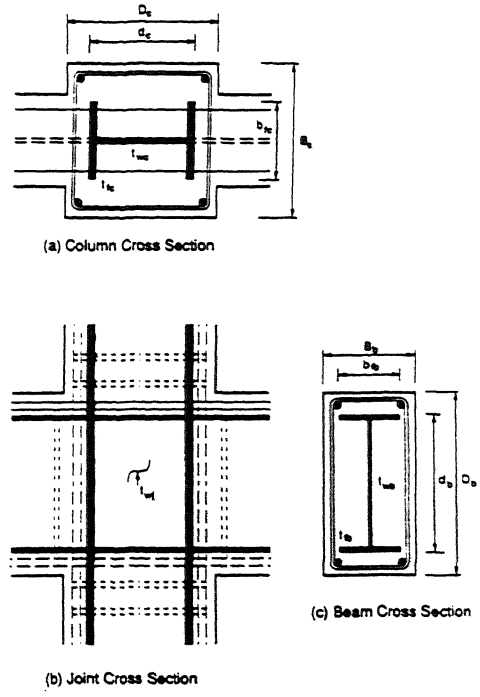

Figure 1. Composite beam-to-column joint.

analytical procedure developed can also be applied to joints involving slab-reinforced steel beams and composite columns. The concept of superposition of the strengths of steel and concrete joint panels has also been adopted.

2.1 Assumptions

The following assumptions have been made in the analysis:

1. The axial and flexural deformations of the joint are neglected since they are relatively small in comparison with the shear deformation. The effect of column axial force, however, is included in the cyclic analysis because of strength deterioration.
2. Local buckling of joint web and flanges are prevented.
3. Tensile strength of concrete is neglected.

2.2 Scope

The composite columns are assumed to contain a sufficiently large steel shape, which would insure satisfaction of the above assumptions. The beams may vary from bare steel to concrete encased with an arbitrary overall width. Only interior joints are dealt with in this paper.

2.3 Analysis for monotonic loading

Figure 2 illustrates the boundary forces on a joint panel and the equivalent joint shear forces. The joint panel boundary forces consist of the bending moments and shear forces of the columns and beams, and the column axial forces. The boundary forces are replaced by an equivalent joint shear force, Q, calculated from equilibrium:

$$Q = \frac{M_{cu} + M_{cl}}{h_c} - 0.5\,(V_{br} + V_{bl}) \qquad (1)$$

Equation (1) may be approximated in terms of the bending moments and shear shear forces of the beams by assuming that $(M_{cu} + M_{cl})$ is equal to $(M_{br} + M_{bl})$,

$$Q = \frac{M_{br} + M_{bl}}{h_c} - 0.5\,(V_{br} + V_{bl}) \qquad (2)$$

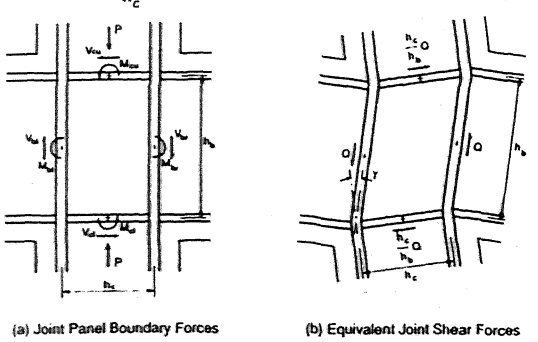

(a) Joint Panel Boundary Forces (b) Equivalent Joint Shear Forces

Figure 2. Boundary forces on joint panels and equivalent joint shear forces.

In this study, the joint shear, Q, given by Eq. (2) and the angular deformation, γ, are used to describe the joint behavior. The joint shear is divided into two parts, Q_s and Q_c for the steel panel and concrete panel, respectively, because the analysis uses the concept of superposition of the two panels.

Figure 3 shows the strength components of a composite joint, separating the contributions of the steel and concrete panels. Based on the observed deformation configurations from the previous tests, it was possible to visualize the failure mechanisms

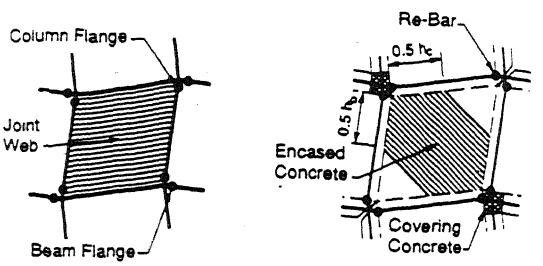

(a) Steel Panel (b) Concrete Panel

Figure 3. Strength components in composite joints.

of the joints and apply the mechanism method to evaluate the limit values of Q_s and Q_c. For the steel panel, the strength is contributed by joint web shear yielding, and formation of plastic hinges in the flanges of the column and beams. The reinforced concrete panel derives its strength from encased concrete diagonal crushing, plastic hinge formation in the reinforcing bars, and covering concrete at the joint corner, which is in closing mode. The corner concrete in opening mode does not contribute to the joint strength since concrete tensile strength is neglected.

2.3.1 Steel panel

Figure 4-(a) shows the proposed monotonic shear vs. angular deformation model for the steel panel. The Q_s-γ relationship consists of two curves, one linear and one hyperbolic. The linear curve with stiffness k_{se} represents the response of the joint web (excluding the contribution of the beam and column flanges). The yield shear, yield deformation, and elastic stiffness are given by

$$Q_{sw} = \frac{F_{yj}}{\sqrt{3}}\, t_{wj}\, h_b \qquad (3)$$

$$\gamma_{sw} = \frac{2\,(1+\nu_s)}{E_s}\,\frac{F_{yj}}{\sqrt{3}} \quad \text{(rad.)} \qquad (4)$$

$$k_{se} = \frac{Q_{sw}}{\gamma_{sw}} = \frac{E_s\, t_{wj}\, h_b}{2\,(1+\nu_s)} \qquad (5)$$

where
F_{yj} = yield stress of joint steel panel
E_s = Young's modulus of steel
ν_s = Poisson's ratio of steel

This linear curve ends at $0.5\,\alpha\,Q_{sn}$, where α is a stiffness degradation factor and Q_{sn} is the nominal strength to be defined later.

The hyperbolic curve representing the nonlinear deformation hardening behavior is expressed as

$$Q_s = \frac{c_1}{\gamma + c_2} + c_3\gamma + c_4 \qquad (6)$$

where the coefficients c_1 through c_4 are to be determined from the following four conditions: (1) continuity with the linear curve at $Q = 0.5\,\alpha\,Q_{sn}$, (2) continuity of the slope with the linear curve, (3) passing through the nominal strength point defined by γ_{sn} and Q_{sn}, and (4) passing through a specific point defined by $\gamma = 4\%$ and $Q_{s,4\%}$ as shown.
Conditions (3) and (4) are discussed below.

The nominal joint strength, Q_{sn}, including the flange plastic hinge moments, is calculated by the mechanism approach as follows:

$$Q_{sn} = Q_{sw} + (F_{ycf} b_{cf} t_{cf}^2 + F_{ybf} b_{bf} t_{bf}^2)/h_c \qquad (7)$$

where F_{ycf} and F_{ybf} are the yield stress of column flange and beam flange, respectively. The corresponding shear deformation, γ_{sn}, is selected by adopting Wang's model (1988):

$$\gamma_{sn} = 3.5\ \gamma_{sw} \qquad (8)$$

The shear force, $Q_{s,4\%}$, at $\gamma = 4\%$ is determined by fitting the available test results and is expressed in terms of Q_{sn} and γ_{sn}:

$$Q_{s,4\%} = Q_{sn}\left\{1 + 0.1\left(\frac{0.04}{\gamma_{sn}} - 1\right)\right\} \qquad (9)$$

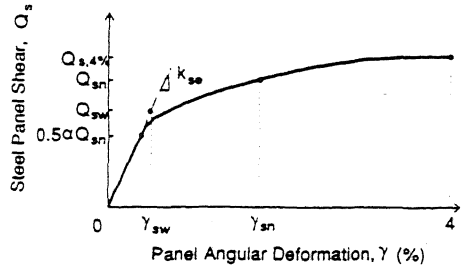

(a) Steel Panel

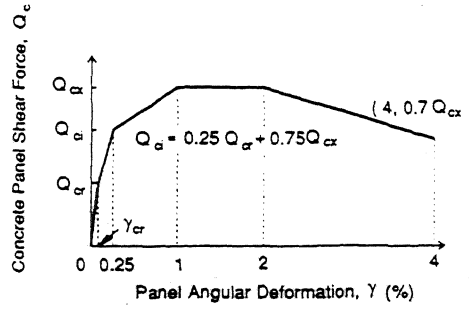

(b) Concrete Panel

Figure 4. Monotonic shear force vs. shear deformation model of composite joint.

2.3.2 Reinforced Concrete Panel

Figure 4-(b) shows the model proposed for the reinforced concrete panel. The first elastic curve considers shear cracking and crack deformation of the panel and assumes that the cracking strength of concrete is equal to 10 % of the crushing strength.

$$Q_{cr} = 0.1\ f'_c\ B_c\ h_b \qquad (10)$$

$$\gamma_{cr} = \frac{2(1+\nu_c)}{E_c}\,0.1\ f'_c \simeq 2.4 \times 10^{-4} \quad (\text{rad.}) \qquad (11)$$

The maximum shear strength, Q_{cx}, is calculated by adding the strength of each of the three components: encased concrete, cover concrete, reinforcing bars.

$$Q_{cx} = Q_{ce} + Q_{cc} + Q_{cb} \qquad (12)$$

The determination of these component strengths will be discussed later.

The other reference points in Fig. 4-(b) are determined empirically by examining the existing test results as follows:
1. The intermediate point between cracking and maximum shear is
$Q_{ci} = 0.25\ Q_{cr} + 0.75\ Q_{cx}$ at $\gamma = 0.25\%$
2. The maximum shear is maintained from $\gamma = 1\%$ to 2%
3. The descending curve passes through the point defined by $0.7\ Q_{cx}$ at $\gamma = 4\%$

The strength of the encased concrete is calculated by taking into account four issues: effective breadth of the concrete panel, b_{fe}, concrete confinement factor, k_j, friction coefficient, μ, between the encased concrete and joint flanges, and the effective width factor, j. The effective breadth of the encased concrete is the column flange width, b_{fc}, for the case of bare steel beams. For the case of encased beams, b_{fe} is taken as

$$b_{fe} = 0.5\ (\ b_{fc} + B_b\ ) \geq b_{fc} \qquad (13)$$

where b_{fc} is the width of steel column flange, and B_b is the width of encased composite beam.

The confinement factor, k_j, of the encased concrete has been selected by examining the bearing strength test results presented by Niyogi (1973).

$$k_j = 2.2 - \frac{b_{fe}}{B_c} \qquad (14)$$

The j factor pertaining to the encased concrete width was found to be for an interior joint. This was based on a deformed shape established by assuming that the boundary flanges's lengths are unchanged and by neglecting the concrete Poisson effect.

The joint shear resistance of the encased concrete can be expressed as

$$Q_{ce} = \frac{(0.5+a)}{(1+a^2)(1+a)} k_j f'_c b_{fe} h_c \quad (15)$$

in which a is the panel aspect ratio, h_c/h_b.

The shear resistances due to cover concrete and reinforcing bars can be calculated by a mechanism approach as follows:

$$Q_{cc} = (B_b h_{bc}^2 + B_c h_{cc}^2) f'_c / h_c \quad (16)$$

$$Q_{cb} = \sum 0.167 r_b^3 F_{yr} / h_c \quad (17)$$

where r_b is the radius of the reinforcing bars in the column and beams, and F_{yr} the yield stress of the bars.

3 HYSTERETIC MODEL FOR JOINTS

The proposed hysteretic shear force-deformation model has been developed empirically by examining the existing experimental results. It's development is described separately for the steel and concrete panels (see Fig. 5).

3.1 Steel panel

The hysteretic Q_s-γ relationship of a steel panel is made up of three curves: one linear elastic curve, and two hyperbolic curves near the two bounding lines. The basic rule specified is that only when deformation reversal occurs on a hyperbolic curve, the linear and the other hyperbolic curve are updated.

The upper limit of the linear elastic deformation range is defined by αQ_{sn}, where α is the stiffness degradation factor and is constant for a specific joint. The two hyperbolic curves near the bounding lines are expressed as

$$Q_s = \frac{c_1}{\gamma + c_2} + c_3\gamma + c_4 \quad (18)$$

where the coefficients c_1 through c_4 are determined using the following four conditions: (1) continuity with the linear elastic curve; (2) continuity of the slope with the linear elastic curve; (3) convergence to the bounding line; and (4) convergency of the slope to the bounding line slope.

The bounding lines are established by considering the following factors as well as the bounding slope and the cyclic steady curve:

- Hardening factor, $F_H = 0.45$
- Softening factor, $F_S = 0.07$
- Mean shear relaxation factor, $F_R = 0.05$
- Slope of shear force bound, $k_s^o = 0.015\ k_{se}$
- Cyclic steady curve, $\frac{\gamma}{\gamma_{sn}} = \frac{Q_s}{Q_{sn}} + \left(\frac{Q_s}{Q_{sn}}\right)^5$

The F_H, F_S and F_R factors are identical to those used in the Cofie's σ-ϵ model (1985), which was developed for A36 steel, but the stress bound slope and the cyclic steady curve have been modified to achieve better agreement with the available test results.

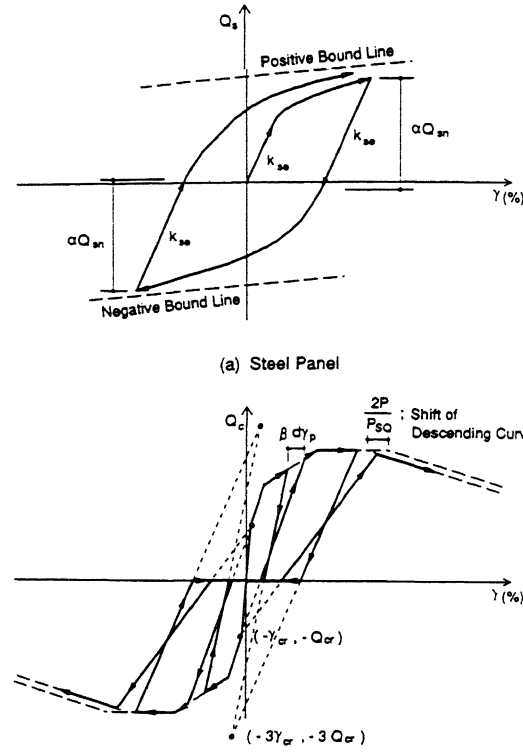

Figure 5. Hysteretic shear force vs. shear deformation model of composite joint.

3.2 Reinforced concrete panel

The hysteretic Q_s-γ relationship of the reinforced concrete panel is defined by multilinear curves as shown in Fig. 5-(b). The envelope of the hysteresis model is identical to the monotonic model except that the descending curve deformation is shifted by an amount equal to $0.02P/P_{SQ}$ to take into account the effect of axial force. P_{SQ} is the squash load of column.

The unloading and reloading curves exist between the envelope and zero force line. The extended line of the unloading and reloading curves at the

positive side passes through the reference points, ($-\gamma_{cr}$, $-Q_{cr}$) and ($-3\gamma_{cr}$, $-3Q_{cr}$), respectively. If a force reversal occurs on the unloading or reloading curve, the Q_s-γ relationship remains on the unloading or reloading curve, respectively. These two reference points are selected to take account of the energy dissipation capacity of the reinforcing bars and the confined concrete.

To account for strength deterioration, the β factor shown in the figure is introduced. The target point of the reloading curve is shifted by the amount of $\beta d\gamma_p$ where $d\gamma_p$ refers to the plastic deformations previously accumulated on the opposite side. A constant β value of 0.05 is adopted by fitting the existing test results.

4 COMPARISON WITH TEST RESULTS

4.1 Monotonic behavior

Figure 6 shows the monotonic behavior of Nishimura's joints (1986) without axial compression on column. There were five specimens with different beam widths, B_b. The experimental and calculated results show good agreement in terms of stiffness, strength, and deformation hardening. The tests indicated that the joint panels were capable of reaching a maximum angular rotation of 0.05 radian in most cases.

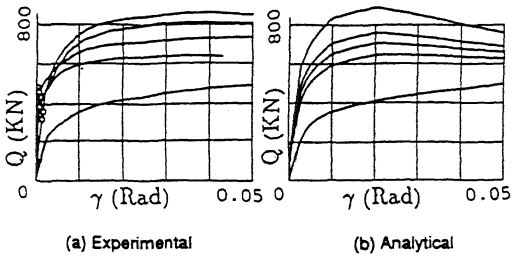

Figure 6. Comparison of experimental and analytically predicted joint behavior (monotonic loading).

4.2 Hysteretic behavior

Figures 7 shows hysteretic behavior of joint panels of Nishimura's specimens (1986)without axial force on column. The experimental and calculated results of the joints show good agreement (except the last few cycles) in terms of stiffness, strength, strength deterioration, stiffness degradation, and pinching behavior. A maximum angular deformation of 0.03 to 0.05 radian was reached in the tests. The results show that composite joints as well as steel beam-to-composite column joints possess considerable ductility and energy dissipation capacity.

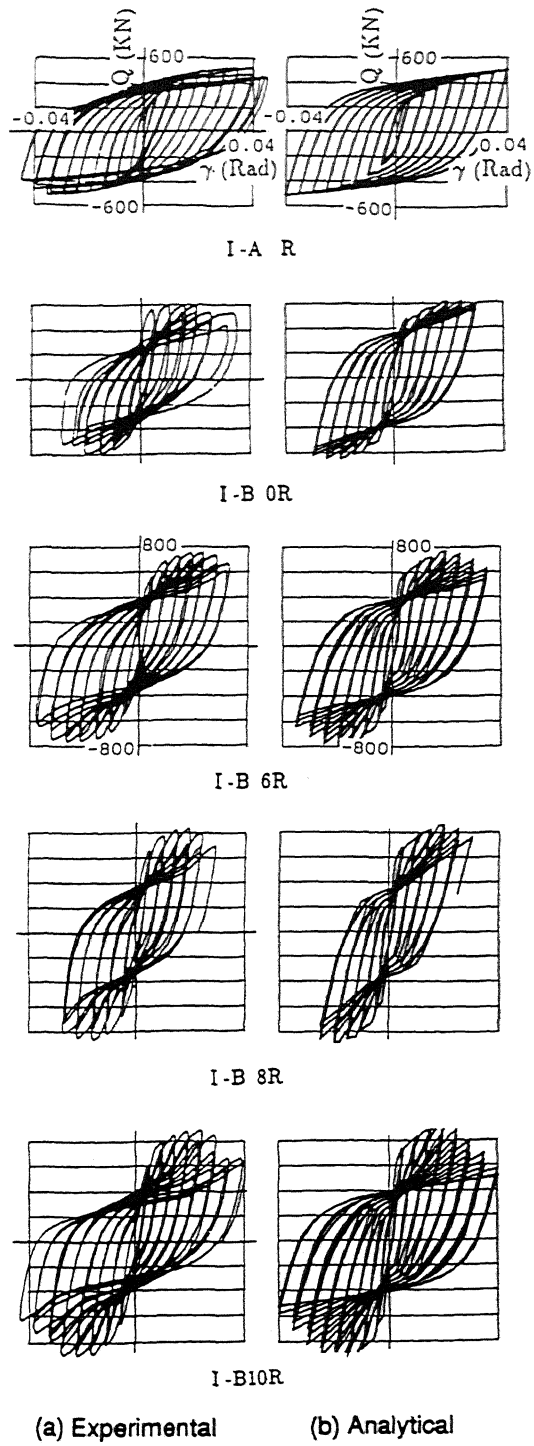

Figure 7. Comparison of experimental and analytically predicted joint behavior (cyclic loading).

5 SUMMARY AND CONCLUSIONS

By employing the superposition method, monotonic and hysteretic joint Q-γ models have been developed for composite beam-to-column joints. During the development of the models, encased concrete behavior has been investigated by defining the effective breadth of the encased concrete beam, the concrete confinement factor, the friction coefficient between encased concrete and joint flanges, and the effective width factor.

In the proposed monotonic model, column axial force effect on joint behavior is neglected based on previous test results. In the proposed hysteresis model, however, column axial force effect is taken into account by shifting the descending curve deformation by an amount equal to $0.02P/P_{SQ}$ based on strength deteriorations observed from the previous experiments.

Both the monotonic and hysteretic models show good agreement with the available test results. These models have already been implemented in inelastic analyses of composite building frame structures subjected to either static lateral loads or earthquake ground excitations (Kim, 1991).

REFERENCES

Cofie, N.G. & H. Krawinkler 1985. Uniaxial cyclic stress-strain behavior of structural steel, J. of *Engineering Mechanics, American Society of Civil* Engineers, III(9): 1105-1120.

Kim, W.K. 1991. Seismic-response analysis and design of composite building structures, Ph.D. dissertation, Lehigh University.

Matsui, C., A. Hamao & M. Wakabayashi 1987. Strength and behavior of SRC beam-to-column connections using high strength steel, Proceedings, International symposium on composite steel concrete structures, Bratislava, Vol.2:27-30.

Minami, K. 1985. Beam to column stress transfer in composite structures. In C.W. Roeder (ed.), Composite and mixed construction, American Society of Civil Engineers: 215-226.

Nishimura, Y., K. Minami & M. Wakabayashi 1986. Shear strength of composite steel and reinforced concrete beam-to-column connection. Trans. Architectural Institute of Japan, 365:87-98.

Nishimura, Y., K. Minami & M. Wakabayashi 1987. Shear strength of composite steel and reinforced concrete joints under axial compression, Japanese structural theses, 33B:211-220.

Niyogi, S.K. 1973. Bearing strength of concrete-geometric variations. J. of Structural Division, American Society of Civil Engineers, 99(ST7): 1471-1489

Wang, S.J. 1988. *Seismic response of steel building* frames with inelastic joint deformation. Ph.D. dissertation, Lehigh University.